ARTICLE OPEN

Check for updates

A ternary heterogeneous hydrogel with strength elements for resilient, self-healing, and recyclable epidermal electronics

Ziya Wang[1,2], Xiuru Xu[1], Yingtian Xu[2], Waner Lin[3] and Zhengchun Peng[1]✉

Epidermal sensing devices, which mimic functionalities and mechanical properties of natural skin, offer great potential for real-time health monitoring via continuous checking of vital signs. However, most existing skin-mounted electronics use a flexible film with high elastic modulus, which hinders physical activity and causes interfacial delamination and skin irritation. The compliance of hydrogel-based devices can firmly conform to complex, curved surfaces without introducing excessive interfacial stresses. However, most hydrogels still suffer from the weakness of stable and reproducible sensing. In this work, we report a skin-friendly epidermal electronic made of a resilient, self-healing, and recyclable polyvinyl alcohol (PVA) hydrogel. The hydrogel is reinforced through a ternary heterogeneous network for good mechanical robustness while maintaining high stretchability and exceptional conformability. Simultaneously, the abundant dynamic hydrogen bonds give the hydrogel rapid self-healing ability. The assembled hydrogel epidermal electronic is able to stably monitor multiple physiological signals as well as sense the strain level of the skin motion and joint bending. The unique, versatile, environmental and biological friendly epidermal electronics will have broad applications in health care, human-machine interface, augmented reality, and so on.

npj Flexible Electronics (2022)6:51 ; https://doi.org/10.1038/s41528-022-00175-7

INTRODUCTION

Epidermal electronics have been providing noninvasive methods to monitor a broad spectrum of vital signs, ranging from electrophysiological activities to heart and respiration rates, and to body's motion, which are closely relevant to normal bodily functions of a person and clinical cues for diseases diagnosis[1]. The continuous real-time acquisitions of body parameters, in a manner that does not disrupt the routine daily activities, are being considered for the human-machine interface as well[2]. Commercial adhesive patches used to fix flexible electronics with high modulus to skin usually cause uncomfortable feelings, skin irritation, and are difficult to detach[3]. Although the strategy of the thinning device[4] and nature inspired microstructural design[5] have been adopted to improve the user experience, the strategies to design a comfortable epidermal device with kind adhesion and detachment, as well as safe and cyclic disposal of electronic wastes have barely been explored[6]. Ideal epidermis-mounted devices should be soft and stretchable to satisfy the conformal integration with skin[7], tenacious, and resilient enough to accommodate the strain induced by body repeated movement[3]. During the past decade, epidermal electronics have been developed by employing serpentine and mesh forms of flexible inorganic electronic materials[8], intrinsically stretchable organic materials[9], and conductive nanomaterials (like Au nanomesh[7], carbon nanotubes[10], and graphene[11]) coating on the ultrathin polymer substrates. Nevertheless, one critical scientific challenge remains, as the aforementioned approaches encounter an irreconcilable contradiction between the ultrathin formfactor and mechanical robustness (usually <50% stretching), which are imperative in epidermal electronics[12]. Meanwhile, the fabrication of epidermal electronics using those materials usually involves photolithography, thin-film deposition, transfer techniques, and other complicated procedures, which are costly and time-consuming[13].

Conductive hydrogel, owing to its superior softness, wetness, responsiveness, and biocompatibility, is being part of the continued endeavor toward building a seamless interface between biology and electronics[14]. The soft (equivalent to skin) and stretchable nature (>200% stretching) of hydrogels allows the minimization of mechanical mismatch with biological tissues compared to ultrathin epidermal electronics[15]. However, few of them are both tough and resilient like living tissues such as muscles[16]. Despite various approaches have been employed to enhance the mechanical properties of hydrogel, such as by constructing double networks, adding nanofillers, mechanical training, etc., the resilience of the strengthened hydrogel is still not satisfactory, particularly in comparison to waterless polymers[17]. As one instance of loading to high strain results in permanent deformation or irreversibly fracture in the epidermal sensing[18]. As ideal bioelectronics, the hydrogel electrodes should demonstrate stronger mechanical robustness and repeatable self-healing ability[19,20]. In our previous work, a highly elastic, room-temperature repairable, and recyclable conductive hydrogel based on dual-crosslinked PVA networks was presented[21]. However, the feeble strength of PVA hydrogel narrowed its wearable applications. The intrinsically contradictory requirements for toughness and resilience make it a big challenge to design a gel with both high toughness[22].

Herein, in order to be both energy-efficient and robust, we aim to develop a PVA hydrogel with strength elements (PVA-S) that combines mechanically resilient and rapidly self-healable by introducing ternary heterogeneous network crosslinking and abundant dynamic hydrogen bonds. Compared to the carbon nanotubes reinforced self-healable materials[23,24] and the various double-network hydrogels with high mechanical strength and/or

[1]Center for Stretchable Electronics and Nano Sensors, School of Physics and Optoelectronic Engineering, Shenzhen University, Shenzhen 518060, China. [2]Shenzhen Institute of Artificial Intelligence and Robotics for Society (AIRS), Shenzhen 518129, China. [3]Department of Micro-Nano Electronics, School of Electronic Information and Electrical Engineering, Shanghai Jiao Tong University, Shanghai 200240, China. ✉email: zcpeng@szu.edu.cn

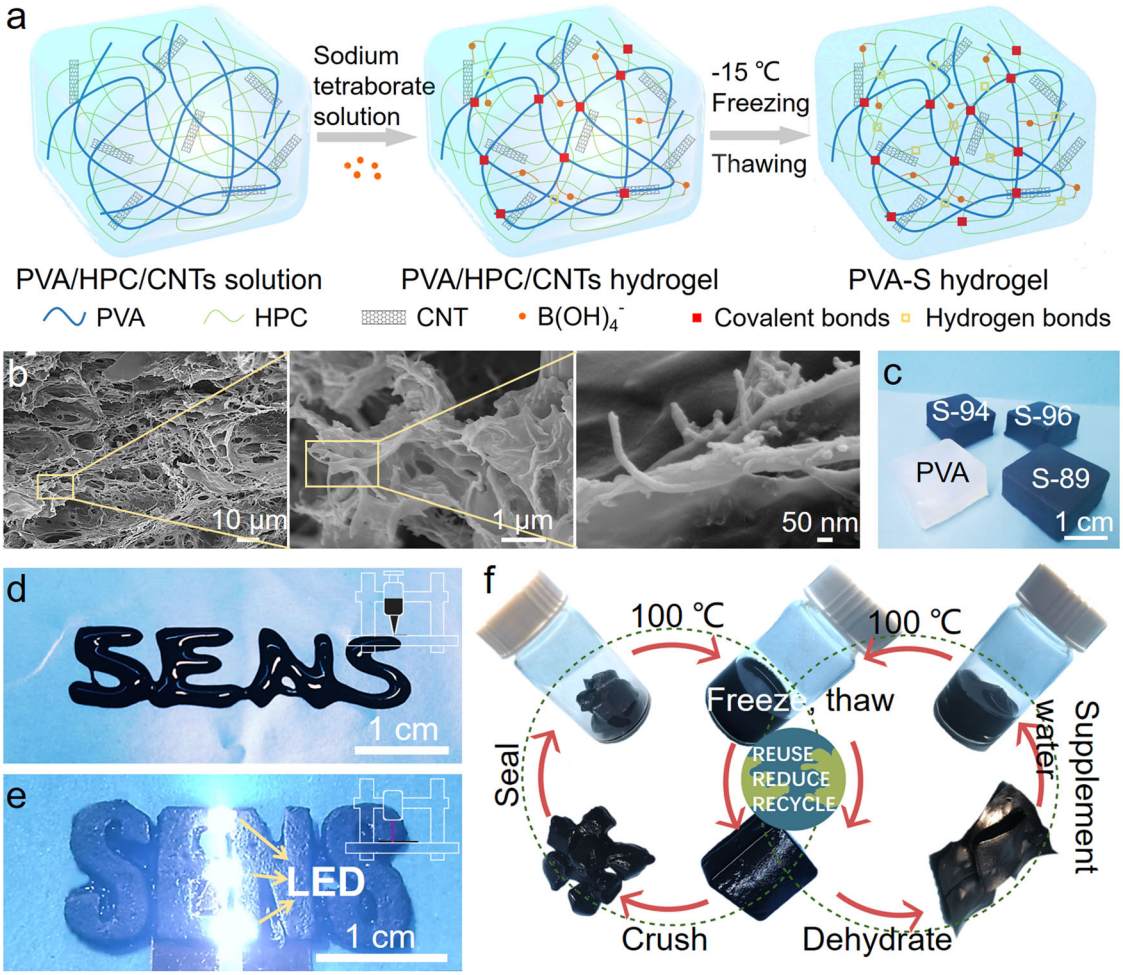

Fig. 1 A tough, self-healing, resilient, conductive PVA-S hydrogel synthesized through a dual-network dual-crosslinking strategy. **a** Schematic diagrams of PVA-S hydrogel fabrication. **b** The microscopic structure of the freeze-dried PVA-S hydrogel at various magnifications. **c** Photograph of typical PVA-S hydrogel bulks fabricated by molding. **d** and **e** Processability and conductivity. The "SENS" figurate hydrogels were obtained by DIW 3D printing and laser engraving, respectively. **f** Recyclability and remoldability. The PVA-S hydrogel fragments (or dehydrated fragments) were fused at 100 °C and remolded.

self-healing[25], the strategy represents an intensive synergistic way of imparting multiple desirable properties into one recyclable functional material. The PVA-S hydrogel is compatible with permeable polytetrafluoroethylene (PTFE) (PP) film, which can strongly adhere to and easily detach from the skin. Hence, epidermal electronics made of these materials will not only have comparable mechanics to the skin but also allow for seamless interfacing with the skin without adversary effect. This new approach of making epidermal electronics represent an economical and eco-friendly technology that can find wide applications in health monitoring and human-machine interface.

RESULTS AND DISCUSSION

Preparation and basic properties of PVA-S hydrogel

A synthetic procedure including three sequential steps was designed to prepare the PVA-S hydrogel with a dual-network dual-crosslinking process (Fig. 1a). Firstly, we employed a PVA hydrogel with tunable modulus as a model material system. Reorganization of the polymer matrix of the embedded hydroxypropyl cellulose (HPC) short-chain fibres and the conductive carbon nanotubes (CNTs) were used to strengthen the mechanical and electrical properties, respectively (Supplementary Fig. 1, 2)[26]. Secondly, the existing PVA molecular chains in HPC/CNTs aqueous system were crosslinked with the chemical crosslinker sodium tetraborate to form an elastic PVA hydrogel (Supplementary Fig. 3)[24]. Thirdly, a freeze-thawed physical crossing procedure was introduced to increase the crystallinity of PVA hydrogel, thereby protecting the integrity of the network, enhancing the anti-fatigue-fracture thresholds, and consolidating the self-healing[27]. The cross-sectional scanning electron microscope (SEM) images of the freeze-dried PVA-S hydrogel in Fig. 1b demonstrates the existed 3D interconnected porous network microstructures. The plentiful interwoven HPC and CNT nanofibers attach themselves to the thin-walled porous architectures during the hydrogel crosslinking process, creating a hierarchical nanofibril architecture. Flourier transform infrared spectroscopy (FTIR) study reveals the interaction between the PVA and other elements and the growing hydrogen bonds in PVA-S compared with unmodified PVA (Supplementary Fig. 4).

Figure 1c–e represent typical examples of the fabricated PVA-S hydrogel which can be easily and freely processed in different shapes by the conventional equal-material and subtractive manufacturing, as well as the popular additive manufacturing, respectively. For example, the desired blocks could readily be achieved by injecting molten PVA-S hydrogel into the customized molds (Fig. 1c). Moreover, the patterned PVA-S hydrogel with "SENS" characters was shaped by the direct ink writing (DIW) 3D printing (Fig. 1d) and the laser engraving (Fig. 1e) respectively,

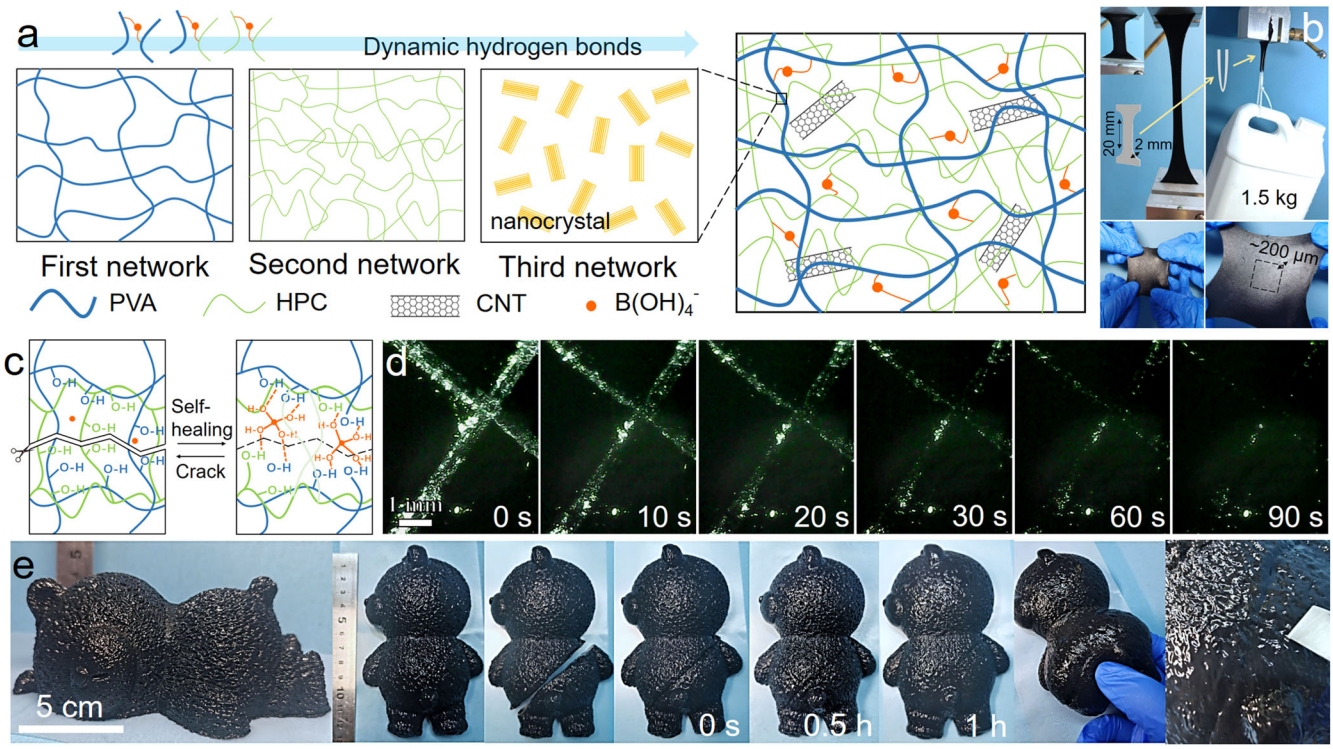

Fig. 2 Mechanical strength and self-healing properties of PVA-S hydrogel. a Schematic mechanism representation of PVA-S hydrogel's ternary strength elements. **b** Outstanding mechanical strength of the PVA-S hydrogel: stretching, lifting test with a load of 1.5 kg and in-plane extension. **c** Schematic illustration of the self-healing mechanism of PVA-S hydrogel. **d** Optical microscopy images of the X-shaped scratch on the PVA-S hydrogel before and after healing for 90 s at room temperature. **e** Massive bear-shaped PVA-S hydrogel (≈15 cm × 8 cm × 5 cm) was cut in half, replaced, and healed adequately for 1 h at room temperature.

confirming their outstanding processability. Another intriguing feature of the PVA-S hydrogel is its recyclable thermal moldability, which allows PVA-S to change its permanent shape as required and recycling. In the demonstration (Fig. 1f and Supplementary Fig. 5), whether the PVA-S hydrogel was chopped into fragments or was fully evaporated, they can be recycled and considered as equivalent to virgin aggregate by placing the segments into a closed container with supplementary water and heating to 100 °C for 2 h. During this period, the segments would be softened and became a sol state. After freezing and thawing, they turned into the desired solid state again and exhibited similar mechanical characteristics after remolding process for several times.

Mechanical strength and self-healing properties

The emerging applications of hydrogels in devices and machines require hydrogels to maintain robustness and resilience under cyclic mechanical loads. The noteworthy difference between PVA-S and normal PVA hydrogel is the unique hierarchical networks comprising mechanically stable nanofibers and abundant dynamical hydrogen bonds. Typical PVA-S sample, consisting of ~ 89 to 96 (wt.%) water and three levels of interpenetrating polymer/nanofibre networks of synergistic strength elements, are mechanically stronger than most of PVA hydrogels with the same water content, as illustrated in Fig. 2a[28,29]. The first network, covalent PVA long-chain strands, are soft and stretchable; while the second network, coiled HPC short-chain strands form tangled porous grids, which were embodied in plentiful micropores into the PVA matrix (Supplementary Fig. 6 and Supplementary Movie 1). To strengthen the concatenating, the conductive CNT nanofibre network was homogeneously penetrated into the polymer. On this basis, as the third strength element, the increase of crystalline domains in cross-linking networks can effectively prevent fatigue crack propagation. Upon tensile force relaxation, the dynamical hydrogen bonds between heterogeneous components and twisting chains could recover to the original condition, contributing to the resilient behaviour simultaneously facilitating reconstruction. As displayed in Fig. 2b, the PVA-S hydrogel can endure large deformations and recovery under more than quadruple uniaxial elongation, triple surface extension, more than 50 N of compression (Supplementary Fig. 7), as well as 1.5 kg of weight without rupture. This reversible stretchability and deformability of PVA-S hydrogel permitted it to adhere to the skin as an epidermal sensing device.

The rapid autonomous self-healing ability at room temperature, which drives important advances in epidermal electronics, particularly with self-healable electrodes as the key enabler[23]. However, most self-healing approaches require the external stimuli (input of energy) or the assistance of a liquid monomer catalyst or solvents[30]. The proposed self-healing mechanism of PVA-S hydrogel was schematically shown in Fig. 2c. The hydrogen bonding between tetrafunctional borate ion and -OH group from PVA and HPC serve as reversible sacrificial bonds, which could break and reform dynamically at room temperature, giving fast self-healing to the ternary heterogeneous polymer networks. The unhindered chain mobility of the hydrogen bonding between the hierarchical nanofibers and nanocrystalline domains is crucial for the formation of resilient hydrogels, which can readily self-healable. The synergistic effect of multiple dynamic chemistries also offers a potential way to recycle the dehydrated PVA-S hydrogel reversibly.

Supplementary Fig. 8 summarized the relationship between elastic modulus and time for sufficient self-healing of the hydrogels concerned in this paper. PVA-S-96 (PVA-S-X, X refers to the weight percentage of water, abbreviated as S-96) with low modulus gives the best self-healing ability, while the PVA-S hydrogel with higher content of PVA/HPC/CNTs shows more

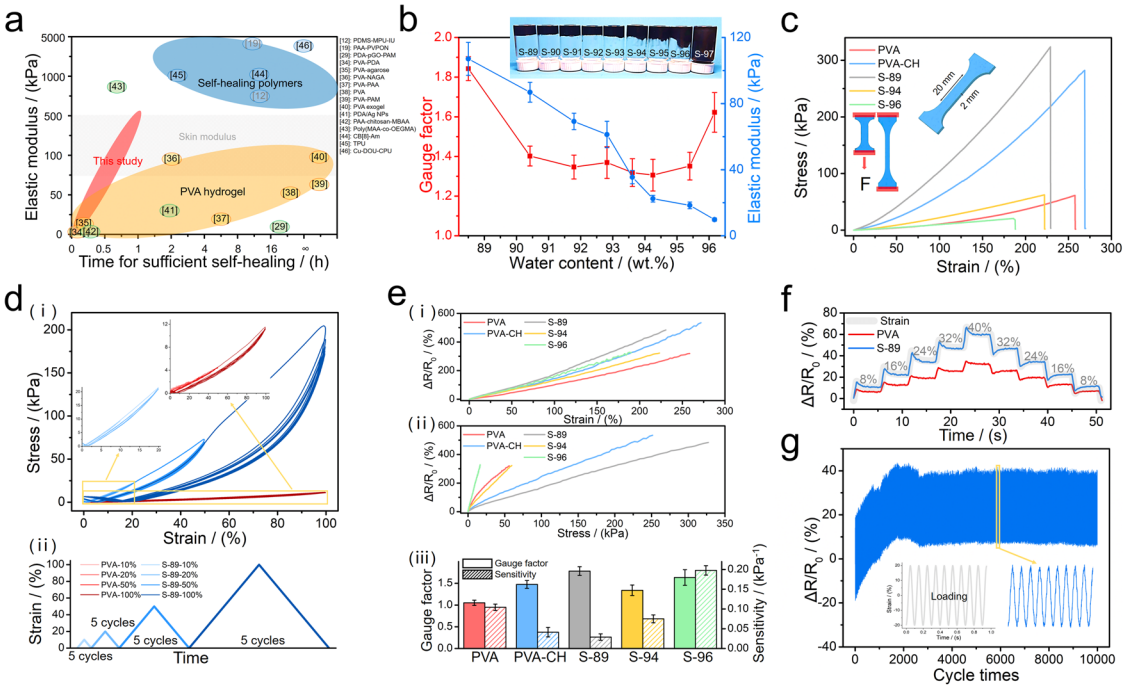

Fig. 3 Experimental evidence of mechanical tolerance and electromechanical properties of the PVA-S hydrogels. a Ashby plot of "elastic modulus" versus "time for sufficient self-healing" of PVA-S and other room-temperature self-healable polymers reported in the literature. **b** Summarized gauge factor and elastic modulus versus water concentration of PVA-S hydrogels. Insets show the PVA-S hydrogels with different water contents adhered at the bottom after flipping the vial for 10 min. **c** The tensile stress-strain curves of representative PVA-S hydrogels. **d** (i) Five successive cyclic tensile loading-unloading curves with different strains of PVA hydrogel and PVA-S hydrogel, respectively. The below figure (ii) shows the applied strain. **e** The electrical resistance variation versus (i) strain and (ii) stress for representative PVA-S hydrogels, respectively. The below figure (iii) calculated the gauge factor and sensitivity, respectively. **f** Resistance variation response curves of the PVA hydrogel and PVA-S hydrogel, respectively, under different static tensile states. **g** The durability test of a PVA-S hydrogel under a 20% strain.

resistance to deformation. The capability to repair physical damage was first evaluated by a scratch recovery test. The microscopic images of PVA-S films with initial ~400 μm wide scratches were shown in Fig. 2d. Because of the superior chain mobility of dynamic hydrogen bonds, the time required for full scratch recovery is only 90 s at room temperatures. Moreover, three representative PVA-S sheets (4 cm × 2 cm × 1 mm) were cut into two completely separated pieces by a razor blade. The short-term self-healing ability was demonstrated again at room temperature after 1 min (Supplementary Fig. 9). Taking about a bulky self-healing behaviour further, the two separated hydrogel halves rejoined seamlessly to heal the "gap" within 1 h (Fig. 2e).

Cyclic stretch-release and electronic test

Because elastic modulus and self-healing of most hydrogels are not compatible with such a large tunable range, from this perspective, the PVA-S hydrogel with a facile fabrication presents clear advantages over the precedent studies on hydrogel materials. Figure 3a summarizes the recent achievements in hydrogels with their self-healing and balanced elastic modulus. The fully listed comparison of related references with their major features are presented in Supplementary Table 2. It should be emphasized that the elastic modulus of PVA-S reached 500 kPa, and the value is estimated to be the highest reported to date for room-temperature fast self-healing PVA hydrogel materials (Supplementary Fig. 8). The highly robust PVA hydrogel is the first introduced ternary heterogeneous HPC/CNTs network (dual-network) with a high crystalline (dual-crosslinking) for reinforced strength and abundant dynamic hydrogen bonding for fast self-healing, simultaneously.

The contents of HPC/CNTs and water in the PVA-S hydrogel are key parameters to modulate mechanical and electrical performances. We conducted a systematical study to investigate the effect of HPC/CNTs ratios on the hydrogels (Supplementary Fig. 2). Summarily, HPC and CNTs synergistically promoted the elastic modulus and gauge factor of PVA hydrogels, but the high content of CNTs significantly retarded the polymerization of the PVA molecular chain and thus easily broken. By comparison, water contents can readily and significantly modulate the mechanical performances of the hydrogel. Based on a synergetic consideration of mechanical and electrical properties, as well as self-healing of hydrogel (Supplementary Fig. 3), as a compromised result, the radio of PVA:CNTs:HPC is 8:1:3, sodium tetraborate is 0.15 wt.%. The recipe was selected in this work to analyze the mechano-electric effect with different water content, considering the relatively high gauge factor up to 1.8, as well as suitable mechanical properties corresponding to human epidermis.

The hydrogel skins exhibit biological tissue-like softness and water content, to avoid mismatch in mechanical properties, coupled with the lack of bio-functionality. As shown in Fig. 3b, a series of polymerizations were carried out, ranging from 89% to maximum, while keeping the same fraction of PVA/HPC/CNTs complexes. The network samples were initially examined by an inverted-vial test. A decrease in viscosity was observed, while stable networks were formed below 96% water content. The elastic modulus of PVA-S hydrogel was reduced since lower network crosslinking density. Nominal tensile stress-strain curves of the representative PVA-S hydrogels (Fig. 3c) demonstrate that the mixed HPC/CNTs porous network leads to strength enhancement and active hydrogen bonding further reinforce the concatenation. To further investigate the viscoelastic properties of the heterogeneous polymer networks, we performed stepwise

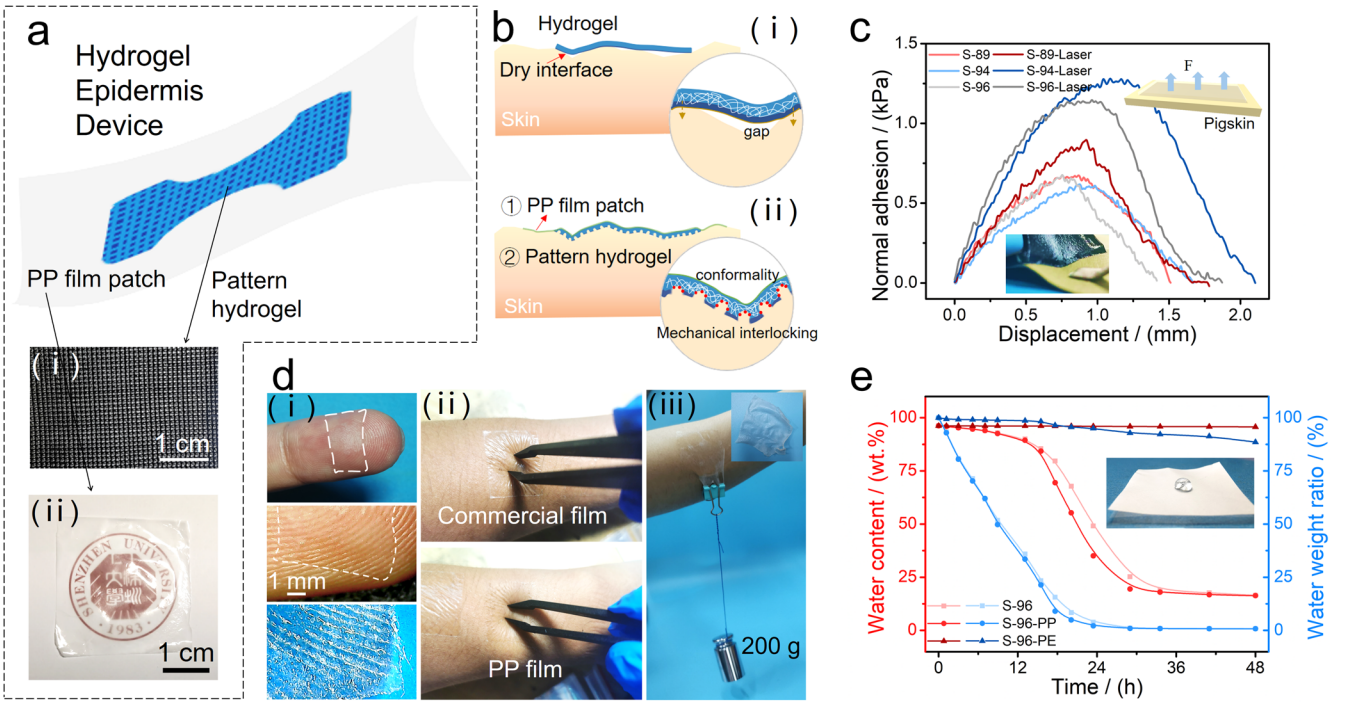

Fig. 4 Schematic illustrations and images of the skin-friendly PVA-S hydrogel and PP film attached to the epidermis. a Schematic illustration of the epidermal device with (i) PVA-S hydrogel electrode and (ii) permeable film. The selective laser engraving of a piece of PVA-S hydrogel to achieve patterns with processed micro-tips (300 μm) surface. **b** The augmented bio-adhesive mechanism of the hydrogel micro-tips. **c** Representative adhesion-force profiles of PVA-S hydrogel attached to a pigskin substrate. Upper inset, schematic of the experimental set-up. Lower inset, photos of the peeling process of a PVA-S hydrogel anchored on a leather. **d** (i) Pictures of a PP film conformally attached to a fingertip. (ii) The PP film on skin compared with a commercial patch under press state. (iii) The demonstration of a PP film (4 cm × 4 cm) fully supporting a 200 g mass on skin. **e** Water vapor permeability of the S-96 hydrogels, S-96 with PP film, and referential S-96 with plastic wrap (PE film) as a function of time. Inset digital images describe the hydrophobic external surface properties of the PP film.

cyclic tensile tests. As shown in Fig. 3d and Supplementary Fig. 10, compared to PDMS and PVA hydrogel, clear yield is observed upon loading the sample to a predetermined strain, PVA-S exhibited more pronounced strain softening residual strain (~ 15%) and mechanical hysteresis (Mullins effect) when retracted to zero stress. It indicates the occurrence of the internal rupture of the brittle HPC/CNTs network in the PVA network. Under the tensile strain, the dynamic and reversible interactions could increase the flexibility of the network by unwrapping and sliding of polymer chains to dissipate energy, whereas the stretchable heterogeneous network remains intact[31]. The response time of the S-89 slightly improved than its initial state due to the growing modulus and cross-linking strengthen (Supplementary Fig. 11).

The large resistance change is highly desired for strain sensing applications, which is a prerequisite for high sensitivity. The electronic properties of PVA-S hydrogel were enhanced by embedding the porous HPC/CNTs second network, which provides more space to facilitate ion migration. Relative resistance changes versus strain/stress are shown in Fig. 3e. PVA-S hydrogels are sensitive to strain and the gauge factor improved almost twice compared with the PVA hydrogel. At the same time, with increasing water content, the sensitivity of PVA-S hydrogels increases. The PVA-S hydrogels exhibited good stability, low noise, and resilience under successive gradient extension test (Fig. 3f). Unlike the conventional conductive elastomer, the PVA-S hydrogel required no additional adhesive tape for adhesiveness. As shown in Supplementary Fig. 12, a piece of hydrogel is directly attached to the skin to detect the bending and touching of the finger knuckle. To simulate the repetitive electromechanical bearing state of PVA-S hydrogel within a period of 1 h, the S-89 sample was endured 10 000 continuous elongation-relaxation cycles at the stretch strain of 20%. As shown in Fig. 3g, based on the unique ternary effects composed of both chemically and physically crosslinked segments, the resistance variation ($\Delta R/R_0$) increased slightly and the mechano-electric curves were almost overlapping after 3 000 cycles (mechanical training), demonstrating the excellent shape-recovery property and outstanding mechanical stability of PVA-S hydrogel. Such results indicate that the PVA-S hydrogel possesses a high potential for skin-mounted motion perception.

Soft, adhesive, and wet hydrogel coatings possess suitability to ensure conformal contact and hydrated epidermis, and therefore, have found a ubiquitous usage in stimulation and recording electrodes of physiological signals[14]. The selective laser engraving process enables the versatile strategy for the patterning of a PVA-S hydrogel electrode, rapidly achieving fresh biomimetic micro-tips with PVA and HPC networks which provide abundant carboxylic acid groups for instant physical cross-links with the tissue surface (Supplementary Fig. 13)[32]. Figure 4a depicts a schematic illustration of the PVA-S hydrogel epidermal electronic (PHEE) prepared by transparent PVA/HPC-PTFE (PP) film (Fig. 4a (ii)) and patterned hydrogel electrode (Fig. 4a(i)) that the excellent shape adaptation of the hydrogel tips to establish intimate contact with the multiscale roughness of the skin (Fig. 4b). The high-adhesion performance of laser engraving microtips originates from more uniform stress distribution and moister surface at the microfibre tip interfaces. As a verification, Fig. 4c shows the vertical adhesion forces-displacement curves of a 1.5 cm × 3 cm sized PVA-S hydrogel with and without laser ablating microtips attached to a pigskin, respectively. The adhesion forces for microtips and unstructured samples (S-94) were 1.3 and 0.6 kPa, respectively, demonstrating significant enhancement of the skin adhesion. To examine the adhesion of PVA-S hydrogel contains tips of different sizes, we measured series of vertical

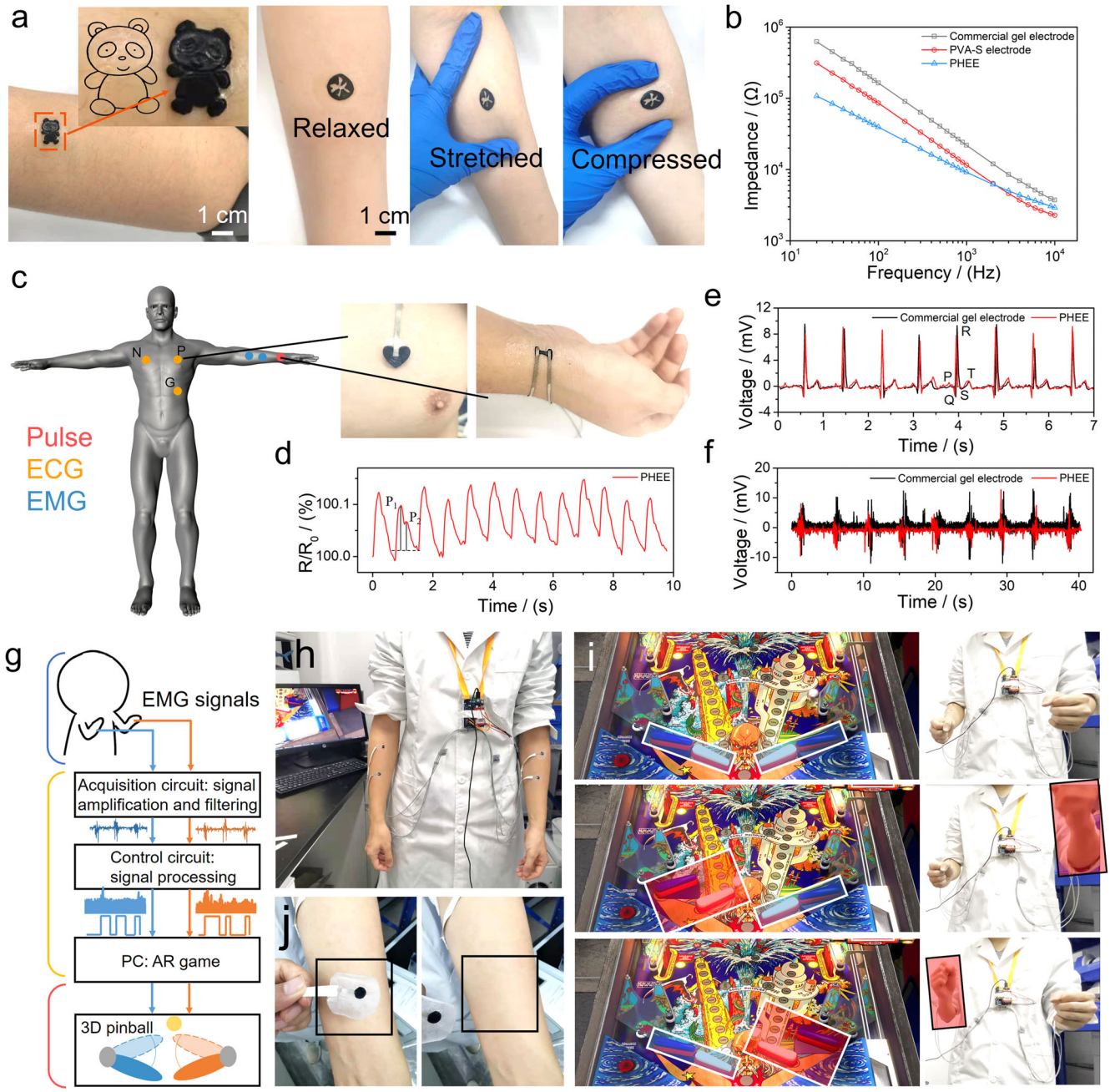

Fig. 5 Schematic illustrations and images of the skin-friendly PHEE for acquiring physiological states. a PHEE mounted on the skin and compressed and stretched by ~ 20%, respectively. **b** The impedance of the skin/electrode interface. AgCl gel commercial electrode with the same area used as reference. **c** Schematic illustration of electrode placement sites. **d** Continuous radial arterial pulse waveform measured on the wrist by the PHEE. **e** ECG response of PHEE compared to commercial gel device. **f** EMG signals measured using the PHEE and commercial gel electrodes, respectively. **g** Overview of the proposed AR control system. **h** Photographs of PHEEs attached to the forearms for AR triggered by the EMG signals. **i** Application in playing 3D pinball with motion sensing. The two pairs of PHEEs correspond to the left and right flippers, respectively. **j** The damage-free and eco-friendly detachment of PHEE after 1 h exercise.

adhesion-force tests summarized in Supplementary Fig. 14. The tips with smaller size and appropriate height can further accelerate the adhesion performance.

In addition to intrinsic conformal adhesion properties from hydrogel mentioned above, a waterproof and breathable covering is another key factor that provides a guard. Strong adhesion during usage and mild detachment afterward are very important aspects for on-skin electronics. The PP film which consists of a porous substrate and water-soluble PVA/HPC adhesive is emerging as a suitable guard film for hydrogel (Fig. 4d and Supplementary Fig. 15). HPC can be prepared in the form of amorphous phase transparent hydrogel with controllable swelling behavior and shape-memory capability, which can be utilized as an adaptable material for reversible adhesives to diverse surfaces with varying roughness[33]. The PVA/HPC adhesive layer, optical micrographs of it on the skin confirm the ultra-intimate coupling between the PTFE and skin (Fig. 4d(i)). Figure 4d(ii) offers a demonstration of the PP film and a commercial adhesive tape (3 M tegaderm film 1623W) which is subjected to various kinds of deformations on the skin, respectively. In contrast to conventional

wearable materials, such as polydimethylsiloxane (PDMS), PP film prominently increases the adhesion force on the skin. The strong attachment between the PP film and the skin can withstand a mass of 200 g (Fig. 4d(iii)). Furthermore, hardly any remnants or irritability were observed on the volunteer's hands after the patch had been attached for 6 h and removed (Supplementary Fig. 16).

The reliability of hydrogel machines becomes critical in daily applications. When a hydrogel electronic is deployed in the human skin, water begins to evaporate, which may result in electronic degradation of the hydrogel machine over time. The daily stability of the PVA-S hydrogel was certified by the fact that there was a tolerable performance degradation after a prolonged place in normal condition (25 °C) for 12 h. The weights of the representative hydrogels were measured at different time intervals (Fig. 4e, Supplementary Fig. 17, 18). The weight and electronic stability of PVA-S hydrogel have very minor drift and it remained moist throughout the day-throw period (12 h). The almost coincidental water content curve with that of the PVA-S hydrogel confirms that PP film has a fully waterproof air and moisture permeable performance. However, the long period operation needs to consider airtight substrate substitutes for PP film (like polyethylene (PE) film in Fig. 4e).

Application as a hydrogel epidermal electronic

Figure 5a offers optical images of the PHEEs with customized patterns on relaxed forearm skin and skin subjected to various kinds of deformations, respectively. Due to applicable modulus, resilience, and micro-tips, the PVA-S hydrogel with PP film can achieve full conformability with human skin easily, even under severe skin deformation (Supplementary Movie 2). Electrode-skin conformability directly dictates the contact impedance which is inversely proportional to the contact surface area. The PHEE-skin interface impedance was measured and compared with the commercial Ag/AgCl gel electrode. PHEE (which has a softer, lighter, and thinner texture) and PVA-S electrodes showed lower impedance value ($|Z|$) owing to the effective interfacial contact area as a result of its malleable and adhesive abilities (Fig. 5b). For instance, the $|Z|$ of the PHEE is 107 kΩ at 20 Hz and 9.2 kΩ at 1 kHz, while those for the commercial electrode are 620 kΩ and 21.9 kΩ, respectively. Conformal contact and low contact impedance are essential for a high signal-to-noise ratio (SNR) in electrophysiological measurements. As shown in Fig. 5c, the gas-permeable PHEEs exhibit outstanding capabilities in recording electrophysiological activities from the skin anywhere and anytime. The single PHEE was attached to the artery of a wrist for real-time monitoring of pulse beats (Fig. 5d). Representative pressure waveforms from radial artery measurement, without signal amplification and postprocessing, consist of two particular components: percussion wave and tidal wave (P1 and P2). Furthermore, high-quality ECG signals were recorded by applying the devices to a volunteer's chest (Fig. 5e). Characteristic ECG peaks (P, Q, R, S, and T) were visible in both sets of data, but the PHEE measurement showed a slightly higher signal magnitude than commercial gel electrodes.

EMG can identify neuromuscular diseases as well as serve as the signals for the augmented reality (AR) and prosthetic control. The electrical activity of the forearm flexor muscle was measured using both the PHEE and commercial gel electrodes, respectively (Fig. 5f). The SNR of the EMG measured by the hydrogel epidermal device (21.8 dB) was higher than that measured by the commercial gel electrodes (18.5 dB). As a transmitter, here we demonstrate the application of a wireless motion sensing game for a human-machine interface. Figure 5g shows an overview of the proposed AR control system, which is composed of three parts: EMG measurement, EMG signal processing, and flipper control. Upon raising the forearm, the electrical potential of the forearm flexor muscle was recorded. It can be compared with a threshold value to identify the muscle state. As a demonstration, a 3D pinball game was used to instantiate this muscular training by improving threshold value regularly (Fig. 5h). The EMG signal of either forearm was assigned with the turning up of left and right flippers to beat the ball, respectively (Fig. 5i). As illustrated in the video (Supplementary Movie 3), the real-time responded EMG signal was highly sensitive, accurate, and bare of delay. Over 1 h of muscular training, more significantly, as a biocompatible skin device, PHEE can be facilely detached without causing skin damage (Fig. 5j).

In summary, we have demonstrated the preparation of a ternary heterogeneous hydrogel with both tough mechanical strength and efficient self-healing ability. Introducing dual-network dual-crosslinking activities and abundant dynamic hydrogen bonds into the PVA hydrogel leads to a synergistic effect among supramolecular polymers, nanofibers, and nanocrystalline domains. With great comprehensive properties including resilience, self-healability, and recyclability, the proposed PVA-S hydrogel is promising as the next-generation material for epidermal electronics. Integrated with a gas-permeable protective film, the epidermal sensing device can strongly adhere to skin for real-time physiological monitoring, and can easily detach from the skin after use. Our findings demonstrate that the PHEE is a promising wearable platform for high-quality vital sign measurement.

METHODS

Synthesis of PVA-S hydrogels

All Poly (vinyl alcohol) (PVA) and PVA-CH hydrogels were synthesized from 8 wt.% PVA solution by a classic freezing-thawing method (physical cross-linking). In a representative PVA-CH precursor solution, 1.0 g carbon nanotube aqueous solution (Aladdin, 9–10 wt.% carbon nanotubes) and 0.3 g Hydroxypropyl cellulose (HPC, Yuanye Bio-technology, 150–400 mPa·s) were fully dissolved in 7.9 g deionized water under stirring at 70 °C for 3 h. Then 0.8 g PVA powder (Sigma-Aldrich, Mw ≈ 130,000, 99 + % hydrolyzed) was added, followed by heating and stirring at 100 °C for 2 h, until all PVA powder had dissolved. The mixture was poured into a mold, frozen at −15 °C for 12 h, and thawed at 25 °C for 4 h. After removal from the mold, the freeze-thawed PVA-CH hydrogels were obtained. Also, the chemical cross-linked PVA-CH hydrogels formed spontaneously within about 10 min after mixing 0.15 wt.% sodium tetraborate ($Na_2B_4O_7$, Aladdin, assay≥99%) with precursor solution. To synthesize double cross-linked PVA-S (S-89) hydrogels, the chemical cross-linked PVA-CH hydrogels were poured into the mold and allowed to cure for 1 h, followed by freezing at −5 °C for 12 h and thawing at 25 °C for 4 h, as the physical cross-linking procedures. By adjusting the water contents of PVA-S, a series of S-X (X refers to the weight percentage of water) hydrogels with various elastic modulus can be designed.

Characterization

The micro-morphologies of the freeze-dried PVA-S hydrogels were investigated by using a field emission scanning electron microscope (FESEM, Hitachi SU-70). Fourier transform infrared spectra (FTIR) of the typical hydrogel samples were recorded on a Thermo Scientific Nicolet 6700 spectrometer.

Mechanical tests

The tensile tests were implemented with the Xie Qiang CTM2010 mechanical testing machine in extension mode. A fixed rate of extension (1 mm min^{-1}) was applied to all tensile testing. The dogbone-shaped sample had the dimensions at an as-prepared state with a width of 10 mm, a thickness of 2 mm, and a gauge length of 20 mm. The nominal stress (σ) was calculated by dividing the applied force (F) by the cross-section area, and the nominal tensile strain (ε) was obtained by dividing stretched length (Δl) by the original length (l_0). The elastic modulus was calculated from the slope over 0-100% strain of the stress-strain curve. Toughness was calculated by the integration area under the stress–strain curves until the fracture point. The compressive mechanical properties of the square shape (20 mm × 20 mm × 10 mm) hydrogels were tested using an Instron E1000 mechanical tester. To investigate the interfacial adhesion of the hydrogels,

a pull-off test was performed using custom-built equipment based on an Instron E1000 mechanical tester. Adhesive patches (size: 1.5 cm × 3 cm) with different hydrogels were attached with a preload of 1 N to the pigskin substrate (30 s) until failure occurred in the pull-off direction. The postmortem pigskins for adhesion tests were obtained from a local market and stored frozen.

Electrical characterizations

The electrical measurements were characterized by an LCR meter (E4980AL, Keysight). To measure the conductivity (σ) of hydrogels (20 mm × 20 mm) by the two-terminal method, two gold foil electrodes (5 mm × 20 mm) were attached to a glass substrate with a 10 mm gap, and the hydrogels were pasted on the electrodes with 1 mm thickness. σ can be calculated by the following equation:

$$\sigma = d/(R \cdot S) \tag{1}$$

where R is the measured value of resistance; S is the sample area between two electrodes and d is the sample thickness.

The electrode-skin impedance was obtained by performing a frequency sweep over a pair of the PVA-S hydrogel epidermal electronic (PHEE) placed adjacent to each other (3 cm) on the wrist. The impedance was recorded by connecting the electrode to an LCR meter through flexible external wiring. Commercial Ag/AgCl gel electrodes and PVA-S hydrogel electrodes (with the comparable surface area) were used for control experiments, respectively.

The electromechanical properties

The dogbone-shaped hydrogels were tested with a tensile tester (CTM2010). Conductive copper foils (3 M 1188) were attached to two ends of the conductive hydrogel for electrical measurements. Resistance recording was conducted in situ by a Keithley 34465 A digital multimeter. All of the strain-resistance characterization steps were conducted in a room environment (25 °C), and the strain rate was set to 1 mm min^{-1}.

Measurement of water content

The hydrogels were placed in an open environment (temperature ≈ 25 °C, relative humidity ≈ 60%) to record the weight during collapsing at predetermined time intervals. Water retention (W_r) of the hydrogels was defined as follows:

$$W_r(\%) = (W_t/W_0) \cdot 100 \tag{2}$$

where W_t is the weight of hydrogel at different intervals during the shrinking process and W_0 was the initial weight of the hydrogel.

Epidermal electronics

Patterned PVA-S hydrogels with processed micro-tips were obtained by laser engraving processing (H-Smart, Huagong Laser). The engraved pattern was designed by AutoCAD. A well-mixed PVA/HPC (3:1) solution was spin-coated on a 4 μm PTFE film at 3000 rpm to obtain the PP film (~ 20 μm). After cured at 60 °C for 4 h, the PP film was cut into a corresponding pattern using laser cutting. To attach the PHEE to the human skin, only spraying several droplets of atomized water to the target position before attaching the hydrogel and PP film in proper order.

Physiological data acquisition

The PHEE was attached to the artery of a wrist for real-time monitoring of pulse beats. A digital multimeter (34465 A, Keithley) was used to record the signals directly, without any signal amplification and postprocessing. ECGs were recorded between the right chest (N-negative) and left chest (P-positive), and a ground electrode on the left upper quadrant. They were then connected to the recording electronics using a conductive fabric tape. The commercial ECG electrode was used as a comparison. The analog front-end AD8232 microchip (Analog Devices) and the Arduino with data logger and Bluetooth modules were used to record the ECG signals. EMG data during tension-relax processes of arm muscle was detected by measuring electromyographic signal through adhered PHEE using an EMG signal acquisition system based on the secondary development of the AD8221 microchip (Analog Devices). Volunteers took part in the experiments following informed consent. The SNRs of ECG and EMG signals for both PHEE and commercial gel electrodes were calculated using the following equation:

$$SNR_{dB} = 20log_{10}\left(\frac{A_{signal}}{A_{noise}}\right) \tag{3}$$

where A_{signal} and A_{noise} refer to the root mean square value of the signal and the noise, respectively.

Demonstration of augmented reality (AR) based on PHEE

The real-time multi-channel EMG signals acquired by the EDK0056 wireless acquisition board filter and amplify the signals from PHEE and send them to Arduino Leonardo's analog pins. Arduino Leonardo used as a microcontroller reads and translates the analog signals as keyboard's push-down and lift-up control signals, and sends them through a pair of Bluetooth to the USB port of the computer. In the 3D Pinball video game, the EMG signals from the left and right forearm flexor muscle correspond to the beating of the left and right flippers, respectively. The voltage acquisition is from continuous circular scanning and processed into time-series on-off signal. When the forearm flexor muscle is tensioned, the EMG voltage signal exceeds the set threshold voltage, triggering off a beating.

Experiments on human subjects

All experiments were conducted under approval from the Institutional Review Board at the Shenzhen Institute of Artificial Intelligence and Robotics for Society.

DATA AVAILABILITY

All relevant data that support the findings of this study are available from the corresponding author on request.

Received: 11 October 2021; Accepted: 10 May 2022;
Published online: 21 June 2022

REFERENCES

1. Ma, Y. et al. Flexible hybrid electronics for digital healthcare. *Adv. Mater.* **32**, 1902062 (2020).
2. Chung, H. U. et al. Wireless epidermal electronic systems with in-sensor analytics for neonatal intensive care. *Science* **363**, eaau0780 (2019).
3. Zhang, Y. & Tao, T. H. Skin-friendly electronics for acquiring human physiological signatures. *Adv. Mater.* **31**, 1905767 (2019).
4. Wang, Y. et al. Epidermal electrodes with enhanced breathability and high sensing performance. *Mater. Today Phys.* **12**, 100191 (2020).
5. Drotlef, D. M., Amjadi, M., Yunusa, M. & Sitti, M. Bioinspired composite microfibers for skin adhesion and signal amplification of wearable sensors. *Adv. Mater.* **29**, 1701353 (2017).
6. Zou, Z. et al. Rehealable, fully recyclable, and malleable electronic skin enabled by dynamic covalent thermoset nanocomposite. *Sci. Adv.* **4**, eaaq0508 (2018).
7. Miyamoto, A. et al. Inflammation-free, gas-permeable, lightweight, stretchable on-skin electronics with nanomeshes. *Nat. Nanotechnol.* **12**, 907 (2017).
8. Kim, D.-H. et al. Epidermal electronics. *Science* **333**, 838–843 (2011).
9. Wang, S. et al. Skin electronics from scalable fabrication of an intrinsically stretchable transistor array. *Nature* **555**, 83–88 (2018).
10. Gogurla, N. et al. Multifunctional and ultrathin electronic tattoo for on-skin diagnostic and therapeutic applications. *Adv. Mater.* **33**, 2008308 (2021).
11. Kabiri Ameri, S. et al. Graphene electronic tattoo sensors. *ACS Nano* **11**, 7634–7641 (2017).
12. Kang, J. et al. Tough and water-insensitive self-healing elastomer for robust electronic skin. *Adv. Mater.* **30**, 1706846 (2018).
13. Sun, B. et al. Gas-permeable, multifunctional on-skin electronics based on laser-induced porous graphene and sugar-templated elastomer sponges. *Adv. Mater.* **30**, 1804327 (2018).
14. Yuk, H., Lu, B. & Zhao, X. Hydrogel bioelectronics. *Chem. Soc. Rev.* **48**, 1642–1667 (2019).
15. Zhao, Y. et al. Ultra-conformal skin electrodes with synergistically enhanced conductivity for long-time and low-motion artifact epidermal electrophysiology. *Nat. Commun.* **12**, 4880 (2021).
16. Liu, R. et al. Highly tough, stretchable and resilient hydrogels strengthened with molecular springs and their application as a wearable, flexible sensor. *Chem. Eng. J.* **415**, 128839 (2021).

17. Wu, S. et al. Poly(vinyl alcohol) hydrogels with broad-range tunable mechanical properties via the Hofmeister effect. *Adv. Mater.* **33**, 2007829 (2021).
18. Cui, J. et al. Synthetically simple, highly resilient hydrogels. *Biomacromolecules* **13**, 584–588 (2012).
19. An, N. et al. Healable and mechanically super-strong polymeric composites derived from hydrogen-bonded polymeric complexes. *Adv. Mater.* **31**, 1904882 (2019).
20. Liu, X., Liu, J., Lin, S. & Zhao, X. Hydrogel machines. *Mater. Today* **36**, 102–124 (2020).
21. Wang, H. et al. A highly elastic, room-temperature repairable and recyclable conductive hydrogel for stretchable electronics. *J. Colloid Interf. Sci.* **588**, 295–304 (2021).
22. Lin, S., Zhou, Y. & Zhao, X. Designing extremely resilient and tough hydrogels via delayed dissipation. *Extrem. Mech. Lett.* **1**, 70–75 (2014).
23. Son, D. et al. An integrated self-healable electronic skin system fabricated via dynamic reconstruction of a nanostructured conducting network. *Nat. Nanotechnol.* **13**, 1057–1065 (2018).
24. Cai, G. et al. Extremely stretchable strain sensors based on conductive self-healing dynamic cross-links hydrogels for human-motion detection. *Adv. Sci.* **4**, 1600190 (2017).
25. Xu, X., Jerca, V. V. & Hoogenboom, R. Bioinspired double network hydrogels: from covalent double network hydrogels via hybrid double network hydrogels to physical double network hydrogels. *Mater. Horiz.* **8**, 1173–1188 (2021).
26. Zhou, Y. et al. Highly stretchable, elastic, and ionic conductive hydrogel for artificial soft electronics. *Adv. Funct. Mater.* **29**, 1806220 (2019).
27. Liu, J. et al. Fatigue-resistant adhesion of hydrogels. *Nat. Commun.* **11**, 1–9 (2020).
28. Rong, Q. et al. Anti-freezing, conductive self-healing organohydrogels with stable strain-sensitivity at subzero temperatures. *Angew. Chem. Int. Edi.* **56**, 14159–14163 (2017).
29. Han, L. et al. A mussel-inspired conductive, self-adhesive, and self-healable tough hydrogel as cell stimulators and implantable bioelectronics. *Small* **13**, 1601916 (2017).
30. Li, C.-H. et al. A highly stretchable autonomous self-healing elastomer. *Nat. Chem.* **8**, 618–624 (2016).
31. Matsuda, T. et al. Mechanoresponsive self-growing hydrogels inspired by muscle training. *Science* **363**, 504–508 (2019).
32. Chen, X. et al. Instant tough bioadhesive with triggerable benign detachment. *P. Natl Acad. Sci.* **117**, 15497–15503 (2020).
33. Yi, H. et al. Ultra-adaptable and wearable photonic skin based on a shape-memory, responsive cellulose derivative. *Adv. Funct. Mater.* **29**, 1902720 (2019).
34. Liu, S. et al. A compliant, self-adhesive and self-healing wearable hydrogel as epidermal strain sensor. *J. Mater. Chem. C.* **6**, 4183–4190 (2018).
35. Chen, W.-P. et al. Hydrogel with ultrafast self-healing property both in air and underwater. *ACS Appl. Mater. Interfaces* **10**, 1258–1265 (2018).
36. Ma, M. et al. A facile strategy for synergistic integration of dynamic covalent bonds and hydrogen bonds to surmount the tradeoff between mechanical property and self-Healing capacity of hydrogels. *Macromol. Mater. Eng.* **306**, 2000577 (2020).
37. Ge, G. et al. Highly stretchable and autonomously healable epidermal sensor based on multi-functional hydrogel frameworks. *J. Mater. Chem. A* **7**, 5949–5956 (2019).
38. Zhang, H., Xia, H. & Zhao, Y. Poly (vinyl alcohol) hydrogel can autonomously self-heal. *ACS Macro Lett.* **1**, 1233–1236 (2012).
39. Ge, G. et al. Stretchable, transparent, and self-patterned hydrogel-based pressure sensor for human motions detection. *Adv. Funct. Mater.* **28**, 1802576 (2018).
40. Xu, L. et al. A solvent-exchange strategy to regulate noncovalent interactions for strong and antiswelling hydrogels. *Adv. Mater.* **32**, 2004579 (2020).
41. Zhao, Y. et al. Skin-inspired antibacterial conductive hydrogels for epidermal sensors and diabetic foot wound dressings. *Adv. Funct. Mater.* **29**, 1901474 (2019).
42. Darabi, M. A. et al. Skin-inspired multifunctional autonomic-intrinsic conductive self-healing hydrogels with pressure sensitivity, stretchability, and 3D printability. *Adv. Mater.* **29**, 1700533 (2017).
43. Jiang, Z., Diggle, B., Shackleford, I. C. & Connal, L. A. Tough, self-healing hydrogels capable of ultrafast shape changing. *Adv. Mater.* **31**, 1904956 (2019).
44. Liu, J. et al. Tough supramolecular polymer networks with extreme stretchability and fast room-temperature self-healing. *Adv. Mater.* **29**, 1605325 (2017).
45. Kim, S. M. et al. Superior toughness and fast self-healing at room temperature engineered by transparent elastomers. *Adv. Mater.* **30**, 1705145 (2018).
46. Zhang, L. et al. A highly efficient self-healing elastomer with unprecedented mechanical properties. *Adv. Mater.* **31**, 1901402 (2019).

ACKNOWLEDGEMENTS

This research was supported by the Science and Technology Innovation Council of Shenzhen (KQTD20170810105439418 and JCYJ20200109114237902), the National Natural Science Foundation of China (61903317), the joint funding program of Guangdong Department of Science and Technology and Hongkong Innovation and Technology (2021A0505110015), the Guangdong Basic and Applied Basic Research Foundation (2021B1515420005), and the funding from the Shenzhen Institute of Artificial Intelligence and Robotics for Society (AC01202101011 and AC01202101106).

AUTHOR CONTRIBUTIONS

The design, preparation, and characterizations of PVA-S hydrogel were completed by Z.W. and X.X.; the demonstrations of the PHEE were carried out by Y.X. and W.L.; Z.W. and Z.P. contributed to the writing of the manuscript; X.X. and Z.P. supervised the overall research.

COMPETING INTERESTS

The authors declare no competing interests.

ADDITIONAL INFORMATION

Supplementary information The online version contains supplementary material available at https://doi.org/10.1038/s41528-022-00175-7.

Correspondence and requests for materials should be addressed to Zhengchun Peng.

Reprints and permission information is available at http://www.nature.com/reprints

Publisher's note Springer Nature remains neutral with regard to jurisdictional claims in published maps and institutional affiliations.